

Cold Gas Measurement System for Linear Aerospike Nozzles

*Original*

Cold Gas Measurement System for Linear Aerospike Nozzles / Bonnet, V., Ortone, F., Di Cicca, G.M., Marsilio, R., Ferlauto, M. - ELETTRONICO. - (2022), pp. 92-96. (2022 IEEE INTERNATIONAL WORKSHOP ON METROLOGY FOR AEROSPACE Pisa, ITALY June 27-29, 2022) [10.1109/MetroAeroSpace54187.2022.9855979].

*Availability:*

This version is available at: 11583/2970155 since: 2022-09-27T06:49:04Z

*Publisher:*

IEEE

*Published*

DOI:10.1109/MetroAeroSpace54187.2022.9855979

*Terms of use:*

This article is made available under terms and conditions as specified in the corresponding bibliographic description in the repository

*Publisher copyright*

IEEE postprint/Author's Accepted Manuscript

©2022 IEEE. Personal use of this material is permitted. Permission from IEEE must be obtained for all other uses, in any current or future media, including reprinting/republishing this material for advertising or promotional purposes, creating new collecting works, for resale or lists, or reuse of any copyrighted component of this work in other works.

(Article begins on next page)

# Cold Gas Measurement System for Linear Aerospike Nozzles

Valentin Bonnet  
*Institut Supérieur de l'Aéronautique et de l'Espace*  
*École Nationale Supérieure de Mécanique et d'Aérotechnique*  
Poitiers, France  
[valentin.bonnet@etu.isae-ensma.fr](mailto:valentin.bonnet@etu.isae-ensma.fr)

Francesca Ortone  
*Department of Mechanical and Aerospace Engineering*  
*Politecnico di Torino*  
Turin, Italy  
[s259914@studenti.polito.it](mailto:s259914@studenti.polito.it)

Gaetano Maria Di Cicca  
*Department of Mechanical and Aerospace Engineering*  
*Politecnico di Torino*  
Turin, Italy  
[gaetano.dicicca@polito.it](mailto:gaetano.dicicca@polito.it)

Roberto Marsilio  
*Department of Mechanical and Aerospace Engineering*  
*Politecnico di Torino*  
Turin, Italy  
[roberto.marsilio@polito.it](mailto:roberto.marsilio@polito.it)

Michele Ferlauto  
*Department of Mechanical and Aerospace Engineering*  
*Politecnico di Torino*  
Turin, Italy  
[michele.ferlauto@polito.it](mailto:michele.ferlauto@polito.it)

**Abstract**— In present work a test rig for cold flow test experiments on linear aerospike nozzles has been designed at Politecnico di Torino. CFD analysis was performed on 2D and 3D aerospike models in order to understand which would be the better inlet nozzle geometry able to work with the designed test-rig mass flow. A time resolved pressure measurement system for the study of flow instabilities has been designed and its dynamic response evaluated.

**Keywords**—aerospike, pressure transducers, CFD

## I. INTRODUCTION

Investigations on innovative propulsion systems is a key element for the forthcoming years to stay competitive in the new space race. The study of nozzle geometry and flow behaviour is fundamental for the rocket nozzle design optimisation. Rocket linear plug nozzles has gathered the interest of propulsion engineers and scientist since 1960's because of their self-adapting capability, which can lead to better performance compared to classical nozzles [1-3]. For high area ratio nozzles with relatively short length, plug nozzles perform better than conventional bell nozzles. However, it should be observed that for equal geometrical area ratios, plug nozzles perform worse at high altitude than conventional bell nozzles because of truncation and clustering [4].

A dedicated infrastructure on which nominal tests can be carried out to study the nozzle characteristics is needed. Having a modular structure which allows to test the nozzles at different scale seems to be crucial for the optimization of nozzle shapes. With this aim a test rig for cold (without high temperature effects) flow test experiments on nozzles has been designed at Politecnico di Torino. The experimental set up adopted is inspired by the design proposed by the ACTiVE project [5].

## II. NOZZLE MODEL DESIGN AND SIMULATION

The test-rig is composed of two subsystems: the air-supply control system and the nozzle model. The first subsystem must provide the prescribed inlet flow conditions and is able to manage interchangeable nozzle models that

may be either axisymmetric, e.g., bell/dualbell nozzle, or two-dimensional, e.g., converging-diverging nozzles and aerospikes. An interfacing duct may be required to generate the correct inlet flow conditions and stream redistribution in the axisymmetric or 2D/3D case. In present work the linear aerospike nozzle model design and setup is addressed. The nozzle contour has been designed by using the method of characteristics as suggested by Angelino [6]. The resulting nozzle flow has been then investigated by CFD. In order to carry out the preliminary design of the test rig equipment, a numerical analysis was performed concerning the aerospike nozzles. The CFD analysis was performed on 2D and 3D aerospike models. The study was addressed to understand which would be the better inlet nozzle geometry able to work with the designed test-rig mass flow. The numerical tool used was Ansys-Fluent. As an example, the 3D geometry tested is represented in figure 1.

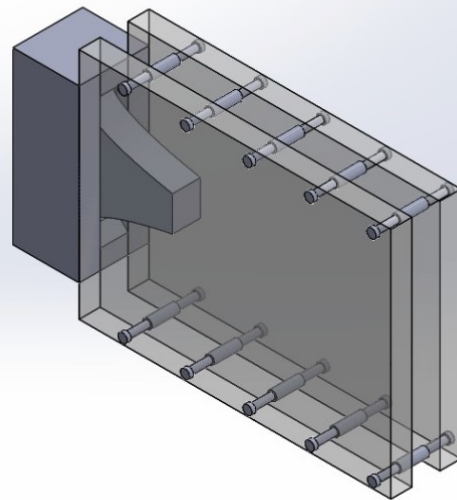


Fig. 1. 3D geometry used to generate the computational domain: 5.5 mm throat height and 40% plug truncation.

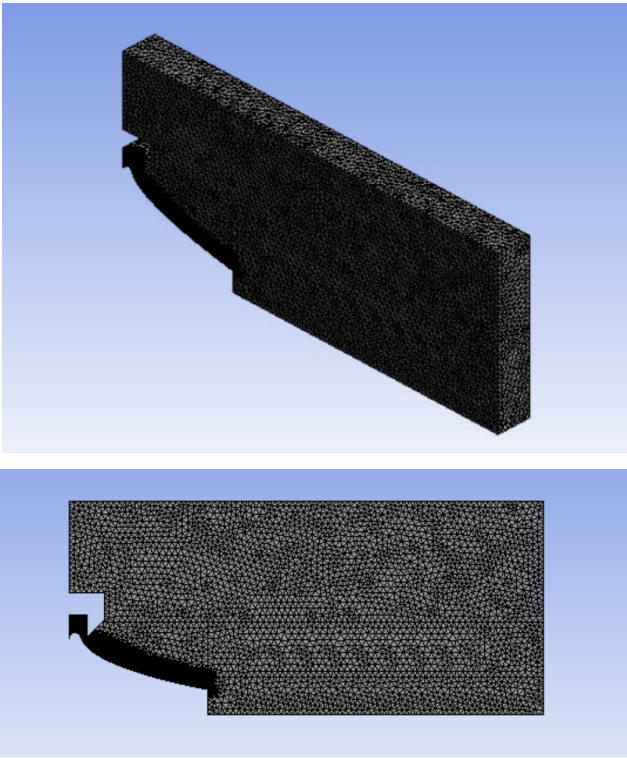


Fig. 2. 3D grid and corresponding computational domain: 5.5 mm throat height and 40% plug truncation.

In Figure 2 is reported the 3D grid with the corresponding computational domain. All the 3D computations were carried out using 512000 cells. The numerical technique is based on the numerical integration of the URANS equations written for compressible flows coupled with Spalart-Allmaras turbulence model. The obtained numerical results were also validated against the experimental ones reported in [4].

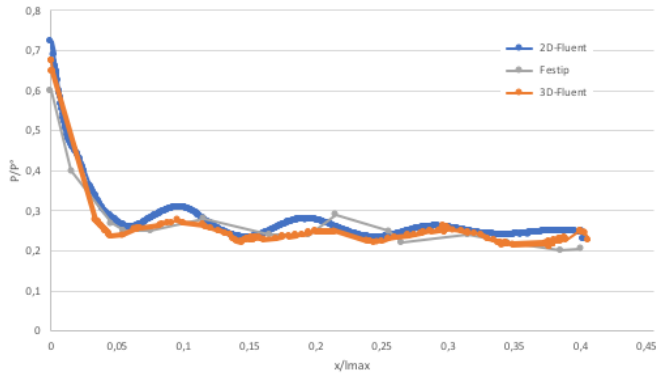


Fig. 3. Aerospike wall pressure distributions.

Figure 3 shows a comparison in term of static pressure between numerical (for 2D and 3D configurations) and experimental (Festip in figure) results. The 3D numerical analysis was performed in order to understand if the presence of walls positioned laterally to the aerospike nozzle (see figure 1) is able to produce huge modifications on the wall pressure distributions along the plug centerline. The computations were performed for a Nozzle Pressure Ratio (NPR, ratio between total pressure  $p_0$  and nozzle exit pressure  $p_e$ ) equal to 4.2 with the nozzle working in over-expanded conditions. The waviness of the pressure distributions highlights the presence of compression and expansion waves in the region close to the plug surface. Both, 2D and 3D numerical results show a very good

agreement with the experimental case. Also, the comparison between the 2D and 3D numerical results evidences that the effects on the wall pressure distribution along the plug centerline due to the presence of the side walls in the 3D case are negligible. Figures 4 and 5 shown the corresponding iso-Mach distributions for 2D and 3D nozzle configurations. From the figure it is clear that even in terms of Mach distribution the 3D effects are negligible as well as for the pressure distribution.

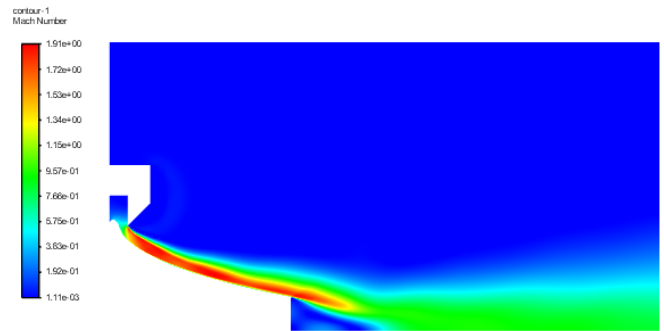


Fig. 4. Mach contour lines for 2D aerospike.

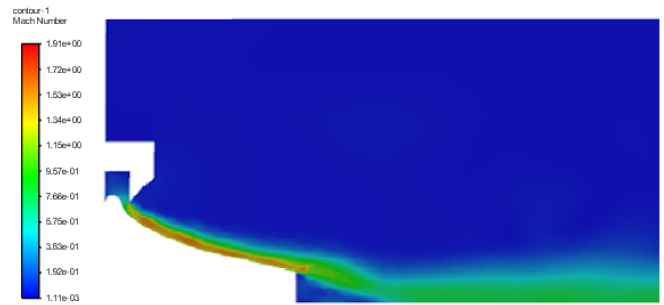


Fig. 5. Mach contour lines for 3D aerospike.

### III. TEST RIG SETUP

The test rig is positioned on a frame, as shown in figure 6. A corrugated metal hose with an inner diameter of 25mm provides the feeding gas (air, with a regulated total pressure  $p_0 \leq 6.5$  bar and a total temperature  $T_0$  of about 288K) and is connected to a diffuser, followed by a flow straightener. A pitot tube which allows to measure the airflow velocity is installed in a downstream conduct.

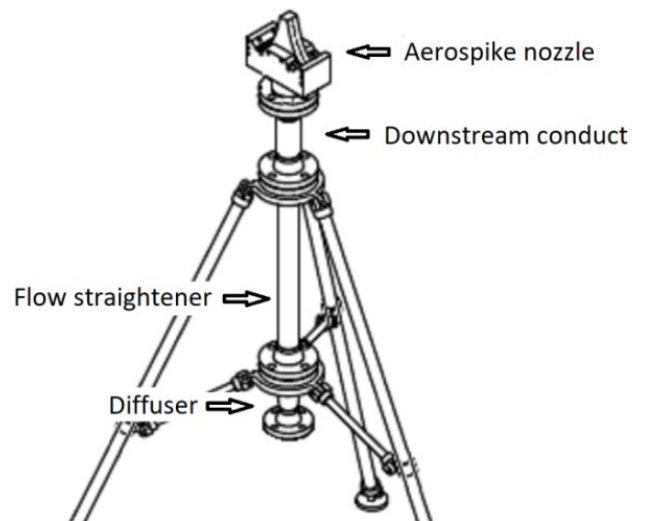


Fig. 6. Sketch of the test rig.

Linear plug nozzles with a width to height throat ratio ( $b/h_t$ ) equal to 6.54 (nozzle 1, see figure 7) and to 30.41 (nozzle 2, see figure 8) can be connected to the flange at the exit of the downstream conduct. For both nozzles the exit Mach number,  $M_e$ , is equal to 1 and the nozzle design pressure ratio  $NPR_d$  is equal to 200. The main characteristic dimensions for the two nozzles are reported in table I.

TABLE I. CHARACTERISTIC DIMENSIONS OF THE NOZZLES

	Nozzle 1	Nozzle 2
Throat height $h_t$	5.5 mm	2.55 mm
Throat width $b$	35.96 mm	77.55 mm
$b/h_t$	6.54	30.41
Throat area $A_t$	395.51 mm <sup>2</sup>	395.51 mm <sup>2</sup>
Exit area $A_E$	5003.21 mm <sup>2</sup>	5003.21 mm <sup>2</sup>
Area ratio $A_E/A_t$	12.65	12.65

The splines describing the plug surfaces of the nozzles have been designed using the method proposed by G. Angelino [6] and a tilt angle  $\theta$  equal to 68.1° has been evaluated at the throat. The plug truncation used is equal to 40% for both nozzles.

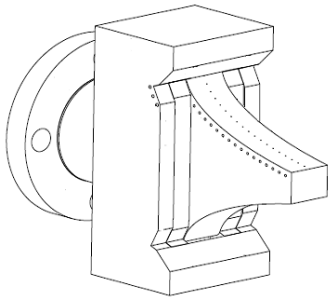


Fig. 7. Sketch of the linear plug nozzle with  $b/h_t=6.54$  and 40% plug truncation (nozzle 1).

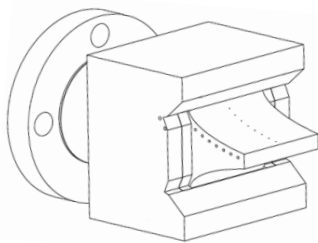


Fig. 8. Sketch of the linear plug nozzle with  $b/h_t=30.41$  and 40% plug truncation (nozzle 2).

Mean and fluctuating pressure distributions are measured in order to characterize the flow evolution along the nozzle plug. For this purpose, pressure ports are positioned along the plug surface.



Fig. 9. Scanivalve® DSA3217-PTP pressure scanner [7].

Mean pressure distributions are measured by means of a Scanivalve® DSA3217-PTP pressure scanner (see figure 9). This unit is capable of measuring up to 16 gas pressures and incorporates 16 temperature compensated piezo-resistive pressure transducers. Also, a 16 bit A/D converter and a microprocessor are included in the unit. The system accuracy is  $\pm 0.05\%$  FS for a pressure range from 5 up to 500 psi. The static wall pressures are measured via orifices (with a diameter is equal to 0.6 mm) drilled perpendicularly to the nozzle plug wall. The distance between two adjacent pressure ports is equal to 7 mm. These ports are connected through small steel tubes and Teflon tubes to the Scanivalve® pressure scanner.

In order to analyse the evolution of flow instabilities, the fluctuating pressure distributions along the nozzle plug are measured by means of piezo-resistive Kulite® pressure transducers type XT-154-190M (see figure 10). These pressure transducers are characterised by a very high natural frequency ( $>150$  kHz without screens).

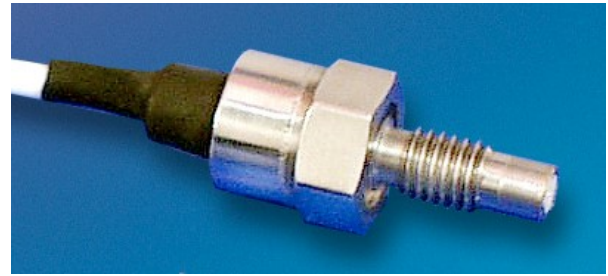


Fig. 10. Kulite® pressure transducers type XT-154-190M [8].

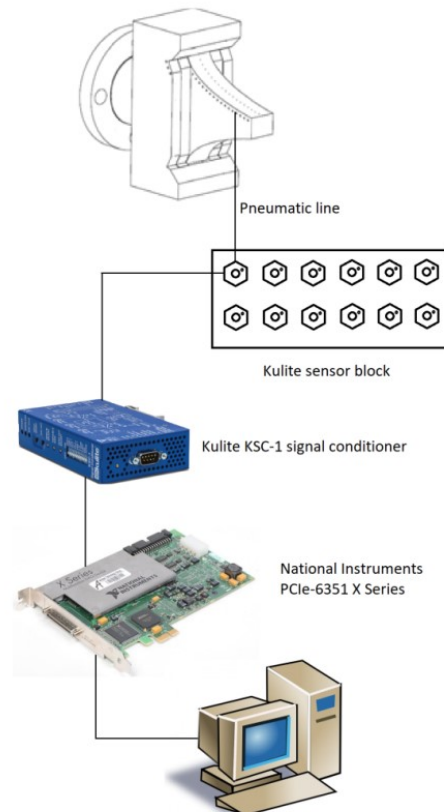


Fig. 11. Fluctuating pressure measurement system scheme.

The pressure ports are connected through small steel tubes and Teflon tubes to the block where Kulite® pressure

transducers are mounted. Pressure transducers are then coupled with Kulite® KSC-1 signal conditioners and a 16bit National Instruments® PCIe-6351 acquisition board. The Kulite® KSC-1 signal conditioners provide the necessary excitation level of 10 V for the sensors. Also, precision 4-pole Butterworth or Bessel low-pass filters are available on this module. Figure 11 shows the scheme for the fluctuating pressure measurement system.

Due to the presence of the pneumatic line used to connect the pressure measurement point and the sensor, the fluctuating pressure measurement system should be carefully designed to minimize amplitude and phase distortion of the pressure signal. In order to evaluate the response characteristics of the pressure measurement system the model proposed by [9] has been considered. In this model the motion of the fluid in a tube with a circular cross-section is described by the Navier-Stokes equations. For a tube of finite length the solution of the linearized flow equations is obtained introducing the following hypothesis: i) sinusoidal disturbances very small; ii) internal radius of the tube small in comparison with its length; iii) laminar flow throughout the system. It was demonstrated that this model allows to predict the response characteristics of the pressure measurement system to a high degree of accuracy.

Each line of the pressure measurement system was modeled as represented in the sketch reported in figure 12. The following geometric parameters characterize the system:

- $D_1 = 0.6$  mm (diameter of pressure port)
- $L_1 = 4$  mm (length of pressure port)
- $D_2 = 1.2$  mm (internal diameter of connecting tube)
- $L_{21} = 35$  mm (length of connecting tube for nozzle 1)
- $L_{22} = 56$  mm (length of connecting tube for nozzle 2)
- $V_v = 49$  mm<sup>3</sup> (pressure transducer volume)

The presence of a discontinuity in tube radius produces remarkable effects on the dynamic response of the system. In particular, it can be observed that a restriction at the entrance of the tube generally yields a reduction of the values of the amplitude ratio. Also, lengthening the pneumatic line results in lower amplitude resonant peaks at smaller frequency values and in higher phase shift for a given frequency.

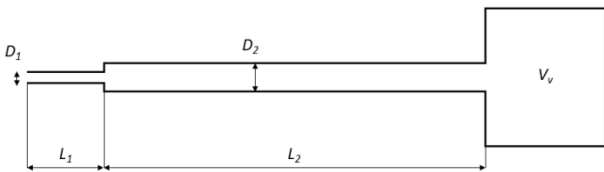


Fig. 12. Sketch of the pressure line with a discontinuity in tube radius.

Due to the mean pressure and temperature distributions along the plug, a suitable transfer function should be used for each pressure transducer used in the system. However, the higher is the mean pressure the lower are the amplitude ratio and phase lag observed for a given frequency. Also, increasing the mean pressure the first resonant peak moves towards higher frequencies. Similar behavior is observed when the mean temperature is increased. In figure 13 the theoretical transfer functions for the pressure measurement

system using piezo-resistive Kulite® pressure transducers type XT-154-190M are shown for the nozzle 1 and two different mean pressure levels. The amplitude and phase spectra are computed for  $p_{\text{mean}}=0.966$  atm and  $p_{\text{mean}}=3.066$  atm that are respectively the minimum and the maximum mean pressures observed along the plug for the case with  $\text{NPR} = 4.2$ . The corresponding mean temperatures are  $T_{\text{mean}}=279$  K and  $T_{\text{mean}}=277$  K respectively. Amplitude spectra show first resonance peaks located at frequencies equal to about 870 Hz and 907 Hz for  $p_{\text{mean}}=0.966$  and  $p_{\text{mean}}=3.066$  atm respectively. Moreover, it can be observed that for frequencies lower than the selected cut off frequency (150 Hz) the errors in evaluating the pressure amplitude and phase are relatively small (always lower than 3.6% for the amplitude and 1.5 degrees for the phase).

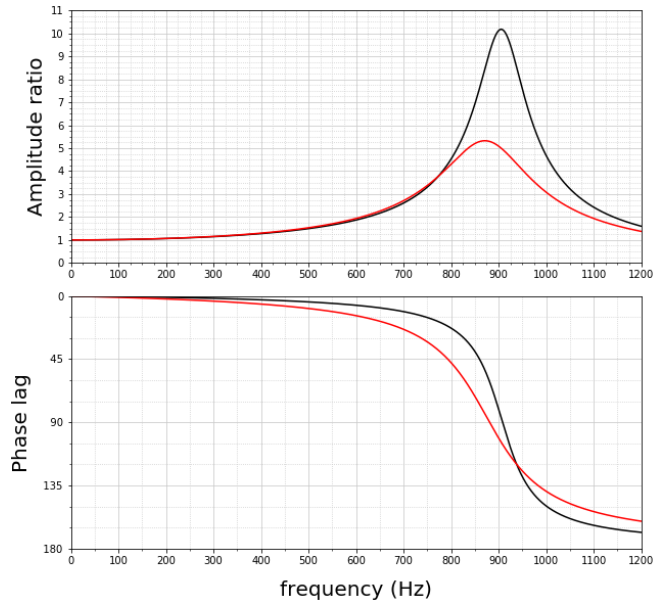


Fig. 13. Amplitude and phase spectra computed for  $p_{\text{mean}}=0.966$  atm and  $T_{\text{mean}} = 279$  K (red line) and  $p_{\text{mean}}=3.066$  atm and  $T_{\text{mean}} = 277$  K (black line). Phase lag in degrees. Nozzle 1.

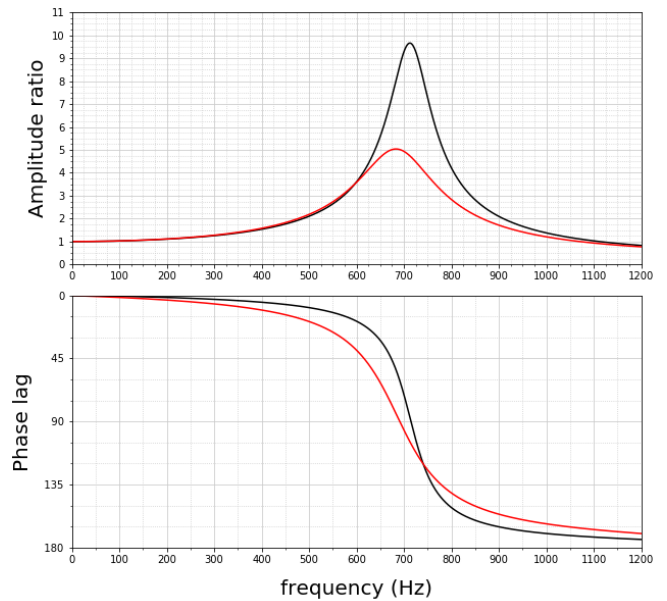


Fig. 14. Amplitude and phase spectra computed for  $p_{\text{mean}}=0.966$  atm and  $T_{\text{mean}} = 279$  K (red line) and  $p_{\text{mean}}=3.066$  atm and  $T_{\text{mean}} = 277$  K (black line). Phase lag in degrees. Nozzle 2.

## REFERENCES

In figure 14 the theoretical transfer functions for the pressure measurement system are shown for the nozzle 2 and the same mean pressure and temperature levels observed for the nozzle 1. Due to the wider throat width of the nozzle 2, the length of the connecting tube must be increased. This results in slightly lower peak amplitudes at smaller frequency values (about 680 Hz and 712 Hz for  $p_{\text{mean}}=0.966$  and  $p_{\text{mean}}=3.066$  atm respectively) and in higher phase shifts. However, for frequencies lower than the selected cut off frequency (150 Hz) the errors in evaluating the pressure amplitude and phase remain relatively small (always lower than 6% for the amplitude and 2.2 degrees for the phase) thus allowing the characterization of large scale flow instabilities with no need of pressure signal corrections.

## CONCLUSIONS

A test rig for cold flow test experiments on linear aerospike nozzles has been designed at Politecnico di Torino. Results from CFD analysis performed on 2D and 3D aerospike models show a very good agreement with the reference experimental case [4] and have been used to validate the nozzle geometries designed for the test rig experiments. The systems for the measurement of the mean and fluctuating pressure distributions along the nozzle plug have been designed and the dynamic response of the pressure fluctuating measurement system has been characterised.

## ACKNOWLEDGMENT

The financial support by the European Community, according to the ERASMUS+ program, is gratefully acknowledged by the first author.

- [1] M. Ferlauto, A. Ferrero, M. Marsicovetere, and R. Marsilio, "Differential throttling and fluidic thrust vectoring in a linear aerospike", *International Journal of Turbomachinery, Propulsion and Power*, 6(2), 2021.
- [2] M. Ferlauto, A. Ferrero, M. Marsicovetere, and R. Marsilio, "A comparison of different technologies for thrust vectoring in a linear aerospike", *World Congress in Computational Mechanics and ECCOMAS Congress*, 2021.
- [3] H. Takahashi, S. Tomioka, N. Sakuranaka, T. Tomita, K. Kuwamori, and G. Masuya, "Experimental Study on the Aerodynamic Performance of Clustered Linear Aerospike Nozzles", *18th AIAA/3AF International Space Planes and Hypersonic Systems and Technologies Conference*, Tours, France, 24–28 September 2012.
- [4] G. Hagemann, H. Immich, T. Nguyen, and G. Dumnov, "Advanced rocket nozzles", *Journal of Propulsion and Power*, 14:620–633, September-October 1998.
- [5] J. Sieder-Katzmann, M. Propst, R. Stark, R. Schneider, S. General, M. Tajmar, and C. Bach, "ACTiVE – Experimental set up and first results of cold gas measurements for linear aerospike nozzles with secondary fluid injection for thrust vectoring", *8th European Conference for Aeronautics and Aerospace Sciences (EUCASS)*, 2019.
- [6] G. Angelino, "Approximate method for plug nozzle design", *AIAA Journal*, 2(10):1834–1835, 1964.
- [7] <http://scanivalve.com/products/pressure-measurement/ethernet-intelligent-pressure-scanners/dsa3217-ptp-pressure-scanner/>
- [8] <https://kulite.com/products/product-advisor/product-catalog/miniature-ruggedized-pressure-transducer-xt-190m/>
- [9] H. Bergh and H. Tijdeman, "Theoretical and experimental results for the dynamic response of pressure measuring systems", *National Aero and Astronautic Research Institute, Amsterdam, Technical Report NLR-TR F.238*, Jan. 1965